Quantitative OCT Angiography of the Retinal Microvasculature and the Choriocapillaris in Myopic Eyes

Al-Sheikh, Mayss ; Phasukkijwatana, Nopasak ; Dolz-Marco, Rosa ; Rahimi, Mansour ; Iafe, Nicholas A ; Freund, K Bailey ; Sadda, SriniVas R ; Sarraf, David

DOI: https://doi.org/10.1167/iovs.16-21289

Quantitative OCT Angiography of the Retinal Microvasculature and the Choriocapillaris in Myopic Eyes

Mayss Al-Sheikh,[1,2] Nopasak Phasukkijwatana,[2,3] Rosa Dolz-Marco,[4] Mansour Rahimi,[2,5] Nicholas A. Iafe,[2] K. Bailey Freund,[4,6] SriniVas R. Sadda,[1] and David Sarraf[2,7]

[1]Doheny Eye Institute, Department of Ophthalmology, David Geffen School of Medicine at UCLA, Los Angeles, California, United States
[2]Stein Eye Institute, Department of Ophthalmology, David Geffen School of Medicine at UCLA, Los Angeles, California, United States
[3]Department of Ophthalmology, Faculty of Medicine Siriraj Hospital, Mahidol University, Bangkok, Thailand
[4]Vitreous Retina Macula Consultants of New York, New York, New York, United States
[5]Department of Ophthalmology, Shiraz University of Medical Sciences, Shiraz, Iran
[6]Department of Ophthalmology, New York University School of Medicine, New York, New York, United States
[7]Greater Los Angeles Veterans Affairs Healthcare System, Los Angeles, California, United States

Correspondence: David Sarraf, Stein Eye Institute, UCLA, 100 Stein Plaza, Los Angeles, CA 90095, USA; dsarraf@ucla.edu.

Submitted: December 13, 2016
Accepted: February 10, 2017

Citation: Al-Sheikh M, Phasukkijwatana N, Dolz-Marco R, et al. Quantitative OCT angiography of the retinal microvasculature and the choriocapillaris in myopic eyes. *Invest Ophthalmol Vis Sci*. 2017;58:2063–2069. DOI: 10.1167/iovs.16-21289

Purpose. To study the retinal capillary microvasculature and the choriocapillaris (CC) in myopic eyes using quantitative optical coherence tomography angiography (OCTA) analysis.

Methods. Macular OCTA images of 3 × 3 mm were obtained using the RTVue-XR Avanti with AngioVue. Quantitative measurements of the retinal capillary microvascular layers and the CC were analyzed using en face projection images. Vessel density and fractal dimension of the superficial and deep retinal capillary plexus, and area and density of flow reduction in the CC were analyzed, quantified, and compared with an age-matched control group.

Results. Fifty eyes with myopia and 34 age-matched healthy eyes were included in this study. The vessel density and the vessel branching complexity using fractal dimension of the retinal capillary microvasculature were significantly lower in myopic eyes ($P < 0.001$ and $P = 0.001$). The total number of flow voids in the CC was lower (108.93 vs. 138.63, $P = 0.001$) but the total and average flow void area was significantly higher (total area 3.715 ± 0.257 vs. 3.596 ± 0.194 mm^2, $P = 0.026$; average area 0.044 ± 0.029 vs. 0.028 ± 0.010 mm^2, $P = 0.002$) compared with the healthy control group. Average choroidal thickness was lower in the myopic group versus the normal control cohort (123.538 ± 73.477 vs. 246.97 ± 41.745 μm, $P < 0.05$) and significantly reduced in eyes with lacquer cracks (LC) compared with myopic eyes without LC formation ($P = 0.003$). There was no correlation between choroidal thickness and quantitative parameters of the CC in the myopic eyes.

Conclusions. The density of the retinal capillary microvasculature is reduced and the area of flow deficit in the CC is increased in eyes with greater myopia. The relevance of microvascular alterations in the setting of myopia warrants further study.

Keywords: myopia, OCT angiography, retinal microvasculature, choriocapillaris, flow void

Optical coherence tomography angiography (OCTA) is a novel noninvasive technology that provides depth-resolved visualization of the retinal and choroidal microvasculature without the need for dye injection[1–3] by using phase or amplitude decorrelation to identify the motion contrast of blood flow. Detailed qualitative and quantitative microvascular information has been studied in various retinal and choroidal diseases using this advanced imaging modality.[4–11]

Myopia is a major cause of legal blindness in many developed countries.[12] In pathologic myopia, elongation of the posterior segment may lead to development of macular complications, including posterior staphyloma, retinoschisis, lacquer crack (LC) formation, chorioretinal atrophy, and myopic choroidal neovascularization (CNV).[13,14] Previous studies using different imaging modalities have demonstrated reduced retinal and choroidal perfusion in high myopia.[15–19] However, current clinical imaging methods are limited in detecting morphologic changes in the choriocapillaris (CC) due to signal attenuation roll-off with greater depth penetration and inability to identify the detailed structure of the choroid and quantify flow within the complex CC.

Previous studies using OCTA have performed quantitative analysis of the CC in healthy and diseased eyes and demonstrated areas of flow void, the size and numbers of which adhere to a systematic pattern of change that correlates with age, degenerative diseases like AMD, and systemic diseases like hypertension.[10,20,21] To our knowledge, choroidal circulation has not been studied in highly myopic eyes using quantitative methods. In the present study, we assessed the microvasculature of the retina and CC in myopic eyes. The superficial and deep retinal capillary plexus and the microvasculature of the CC were quantitatively analyzed with OCTA and compared with an age-matched normal control group. Choroi-

dal thickness and refractive error were also assessed and correlated with the CC changes.

Methods

This study was approved by the Institutional Review Board of the University of California Los Angeles and the Western Institutional Review Board (Olympia, Washington, USA) and conducted in accordance with the ethical standards stated in the Declaration of Helsinki. The study was carried out in accordance with Health Insurance Portability and Accountability Act. Written informed consent was obtained from all examined patients and volunteer participants before OCTA imaging.

Subjects with high myopia and a refraction of greater than –6 diopters (D) or axial lengths longer than 26.5 mm were included in this study.[22] Any patient with a history of prior vitreous or retinal surgery or evidence of retinal disease (other than myopic degeneration) affecting the retinal or choroidal vasculature by history or examination was excluded from the study. Eyes with diffuse RPE atrophy due to high myopia or any structural changes, including myopic CNV that could cause shadowing over the CC were excluded from this quantitative analysis.

Age-matched healthy individuals without any visual symptoms and without any history of previous ocular or systemic diseases were eligible for this study. Patients with vision complaints or a history of surgical intervention (including refractive surgery) or eyes with refractive error greater than 2.5 D or evidence of a retinal disorder were excluded from the normal cohort analysis.

Image Acquisition

The OCTA images were obtained using a spectral-domain OCT device (RTVue-XR Avanti, version 2016.1.0.26; OptoVue, Inc., Fremont, CA, USA). Split-spectrum amplitude-decorrelation angiography was used to extract the OCTA information.[3] The device operated with a central wavelength of 840 nm, an acquisition speed of 70,000 A-scans per second, and a bandwidth of 45 nm. The 3 × 3-mm scans were captured with each cube consisting of two repeated volumes of 304 B-scans. Two orthogonal OCTA imaging volumes were captured to perform motion correction and to minimize motion artifacts arising from microsaccades and changes in fixation during acquisistion.[23,24] Automatic segmentation was performed by the viewing software to generate en face projection images of the superficial retinal capillary plexus (SCP), deep retinal capillary plexus (DCP), and the CC. The SCP en face OCTA image was segmented with an inner boundary 3 μm below the internal limiting membrane and an outer boundary 15 μm below the inner plexiform layer. The DCP en face OCTA image was segmented with an inner boundary 15 μm below the inner plexiform layer and an outer boundary 70 μm below the inner plexiform layer. The CC en face OCTA image was derived by the viewing software with a slab 10-μm thick starting 31 μm deep to the RPE–Bruch's membrane complex. Based on a previous publication, we adjusted this slab with a start level at 34 μm deep to the RPE–Bruch's membrane complex with the same slab thickness to minimize projection artifacts.[25] A cutoff value of signal strength index was set at $\geq$40.[26,27] All scans were reviewed to ensure correct segmentation and sufficient image quality. Any image with a double vessel pattern, motion artifacts, and/or segmentation errors extending more than three lines was excluded.

Image Analysis

The raw images from the SCP, DCP, and CC were exported from the OptoVue software and then imported into the freely available FIJI software (an expanded version of ImageJ version 1.51a; fiji.sc). Vessel density (VD) in the SCP and DCP as caliber per area was calculated on the binarized images as a ratio of the area occupied by vessel in the total 3 × 3 mm image area. The binarization was done with intensity thresholding with Otsu's thresholding method as implemented in ImageJ (http://imagej.nih.gov/ij/; provided in the public domain by the National Institutes of Health, Bethesda, MD, USA). Otsu's method assumes that the image contains two classes of pixels following a bimodal distribution. It calculates optimum threshold by minimizing intraclass variance and maximizing interclass variance.[28] Fractal dimension (FD) as a measure of branching complexity was analyzed using the box-counting method with Fractalyse (ThéMA, Besançon Cedex, France).[29] The box-counting method consists of dividing an image into square boxes of equal sizes and counting the number of boxes containing a vessel segment.[11] The process is repeated several times with boxes of different sizes. The FD value varies with the distribution of vessels in the image and has a value between 0 and 2. The more complex the pattern, the higher the measured value.

In the CC, areas with absent flow signals, so-called flow voids, were identified by thresholding and then measured. The images of the CC in healthy eyes were first qualitatively assessed for the dark no-flow area. Absence of flow was confirmed with analysis of the corresponding cross-sectional B-scan flow overlay (Fig. 1). Areas with no corresponding flow were manually outlined in original 3 × 3-mm scans, and the area in micrometers was calculated as ([pixel of flow void area] × [3/304]^2). The mean flow void area size was measured in all the healthy eyes and an average size of 20 pixels^2 (equal to 0.0002 mm^2; 2000 μm^2) was set as a threshold for the area of no flow. In the next step, the CC raw images were thresholded by using automatic local thresholding with the Phansalkar method and a radius of 15 pixels as implemented in FIJI.[30] The Phansalkar method was used based on a previous publication to select darker regions in potentially low-contrast images.[10] The thresholded images were then analyzed regarding the flow void area using the "Analyze Particles" tool as implemented in FIJI software to count the areas of the thresholded no-flow and to calculate their number, and total and average area.

For the quantitative analysis, eyes with CNV were excluded to eliminate artifact from the shadowing effect of the myopic CNV over the CC, which could result in overestimation of the flow void area.

The choroidal thickness was measured on B-scan OCT (SPECTRALIS; Heidelberg Engineering, Heidelberg, Germany) using a built-in caliper tool in Heidelberg Eye Explorer v1.9.10.0 software (Heidelberg Engineering). Choroidal thickness was defined as a perpendicular distance between the Bruch's membrane and the choroidal scleral junction and was measured at the center of the fovea.

Myopic CNV was identified on fluorescein angiography (Carl Zeiss Meditec, Jena, Germany; SPECTRALIS, Heidelberg Engineering; Topcon Medical Systems, Oakland, NJ, USA; Optos, Dunfermline, UK). The presence of LC as breaks in the RPE–Bruch's membrane complex was confirmed using fundus autofluorescence (SPECTRALIS; Heidelberg Engineering).

Statistical Analysis

The Kolmogorov-Smirnov test was used to evaluate the normal distribution. Independent samples *t*-test was used to compare

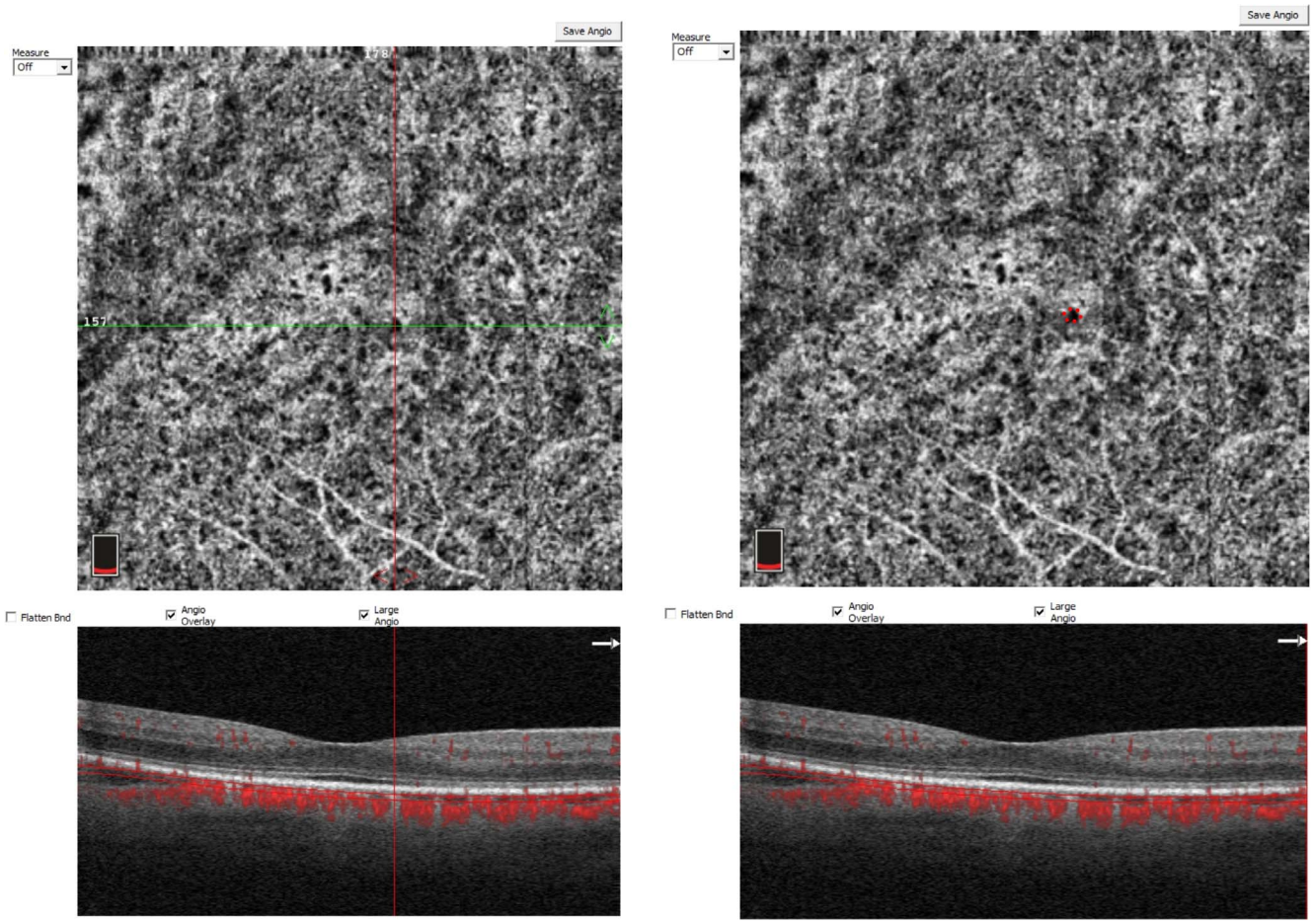

Figure 1. Quantification of flow void area in the CC using en face OCTA and corresponding cross-sectional OCT B-scan with angio overlay. *Upper left*, en face OCTA image of the CC. Lower left, corresponding cross-sectional B scan with segmentation level and angio overlay. The *red* and *green lines* intersect at a dark area, or flow void, and the corresponding B-scan flow overlay illustrates absence of a flow signal. *Upper right*, manual outline of the flow void area in *red*. The flow void area in micrometers was calculated using the following formula: ([pixel of flow void area] × (3/304)^2). Then the "Analyze Particles" command, which measures and counts all the thresholded areas where there is lack of flow, was performed.

the patient group with the age-matched control group. The nonparametric Mann-Whitney *U* test was used for parameters with skewed distribution. We used multivariable linear regression analysis to assess the relationship between quantitative parameters of the CC as independent variables and choroidal thickness as well as refractive error as dependent variable. We also performed a linear regression analysis to study the influence of signal strength on quantitative features of the CC. Discriminant analysis was used to compare the quantitative CC features with LC presence as a categorical value. Statistical Package for Social Science (SPSS) version 21 (SPSS, Inc., IBM Corporation, Chicago, IL, USA) was used for statistical analysis. A $P < 0.05$ was considered significant.

Results

Fifty eyes of 28 patients (15 female, 13 male) with myopia were included in this study. The mean age was 57.00 ± 17.93 years (range, 25–83). The refractive error was –8.29 ± 2.94 D (range, 6–16) after excluding the 13 eyes that underwent cataract or refractive surgery. The mean visual acuity at baseline was 20/30. Thirty-four eyes of 20 age-matched healthy individuals (14 female, 6 male) were included. The mean age was 56.05 ± 19.27 years (range, 27–83) ($P = 0.927$). The refractive error was –0.04 ± 1.06 D (range, 2 to –2). For quantitative measurements in the patient group with myopia, 43 eyes were included after excluding eyes with myopic CNV.

The mean VD ratio in the SCP and DCP is shown in Table 1. In both capillary plexuses, the VD in myopic eyes was statistically significantly lower ($P < 0.001$). Similarly, the FD in the SCP and DCP was statistically significantly lower in both layers (SCP $P < 0.001$, DCP $P = 0.001$).

In the CC, in the total 3 × 3-mm scan there were 108.93 flow voids in the myopic eyes versus 138.63 in the control group ($P = 0.001$). The total area of flow void was 3.715 ± 0.257 mm^2 in the myopic eyes and 3.596 ± 0.194 mm^2 in the control group ($P = 0.026$). The average flow void area was

Table 1. Vessel Density and FD of the SCP and DCP in the Myopic Group Versus the Healthy Age-Matched Control Group

	Myopic Eyes	Control Group	*P*
VD, ratio			
SCP	0.280 ± 0.043	0.325 ± 0.028	< 0.001
DCP	0.327 ± 0.039	0.366 ± 0.032	< 0.001
FD			
SCP	1.571 ± 0.031	1.594 ± 0.016	< 0.001
DCP	1.603 ± 0.039	1.624 ± 0.013	0.001*

* Using nonparametric test, Mann-Whitney *U* test.

Table 2. Quantitative CC Findings Including Total Number of Flow Voids, Total Flow Void Area, and Average Flow Void Area in Myopic Versus Healthy Age-Matched Control Groups

	Myopic Eyes	Control Group	*P*
Total number of flow voids	108.93 ± 45.567	138.63 ± 30.713	0.001
Total flow void area, mm²	3.715 ± 0.257	3.596 ± 0.194	0.026
Average flow void area, mm²	0.044 ± 0.029	0.028 ± 0.010	0.002*

* Using nonparametric test, Mann-Whitney *U* test.

0.044 ± 0.029 mm² in the myopic eyes and 0.028 ± 0.010 mm² in the control group ($P = 0.002$, Table 2; Fig. 2).

The mean subfoveal choroidal thickness was 123.538 ± 73.477 μm (range, 20–309 μm) in the myopic eyes and 246.97 ± 41.745 μm (range, 187–346 um) in the control group ($P < 0.05$).

Choroidal thickness as a dependent variable was correlated with various quantitative parameters using a multivariable linear regression analysis. As expected, there was a significant negative correlation with age ($R = -0.520$, $P < 0.001$; Fig. 3) and a negative correlation with refractive error ($R = 0.402$, $P = 0.025$; Fig. 3). However, choroidal thickness did not correlate with any of the quantitative parameters of the CC.

The association between refractive error as a dependent variable and quantitative features of the CC showed a weak positive correlation with total flow void area and average flow void area, but the difference was not statistically significant (total area of flow void: $R = 0.201$, $P = 0.110$; average flow void area: $R = 0.165$, $P = 0.158$) (Fig. 4).

Of the 51 eyes with myopia, 5 demonstrated LC formation and 7 demonstrated CNV. The discriminant analysis test showed a significant correlation between the total flow void area in the CC and the presence of LC ($P = 0.017$), but no correlation with the average flow void area ($P = 0.104$). Within the group of myopic eyes, the choroidal thickness in eyes with LC formation was significantly less than in those without LC formation ($P = 0.003$).

The signal strength score was 59.00 ± 10.55 in the group of myopic eyes and 66.74 ± 10.92 in the control group ($P = 0.006$). The multivariable linear regression test did not show any association between the signal strength score and the quantitative parameters of the CC (all $P > 0.05$).

Discussion

Optical coherence tomography angiography is a new imaging technology that provides more detailed morphologic microvascular information and greater quantitative capability in various retinal and choroidal diseases. In this study, we used OCTA to analyze and quantitate the density of the retinal capillary plexus and the area of flow reduction in the CC in myopic eyes versus a healthy age-matched control group. We also studied the association between choroidal thickness and flow reduction in the CC within the group of myopic eyes, and correlated this with the presence of myopic complications, including LC.

This study demonstrated a reduced VD in the SCP and the DCP in the myopic group versus the age-matched healthy cohort. Our findings are consistent with previous studies using other techniques.[17,31] Shimada et al.[17] found reduced retinal blood flow in high myopia using laser blood flowmetry. They attributed the reduced blood flow to narrowing of the retinal vessel diameter. Shimada et al.[17] also reported that the velocity of blood flow within the vessel was unchanged in myopic eyes. These findings, supported by our study, may indicate that the microvasculature of the retina may be stretched, leading to reduced VD rather than frank loss. Tokoro[31] reported similar

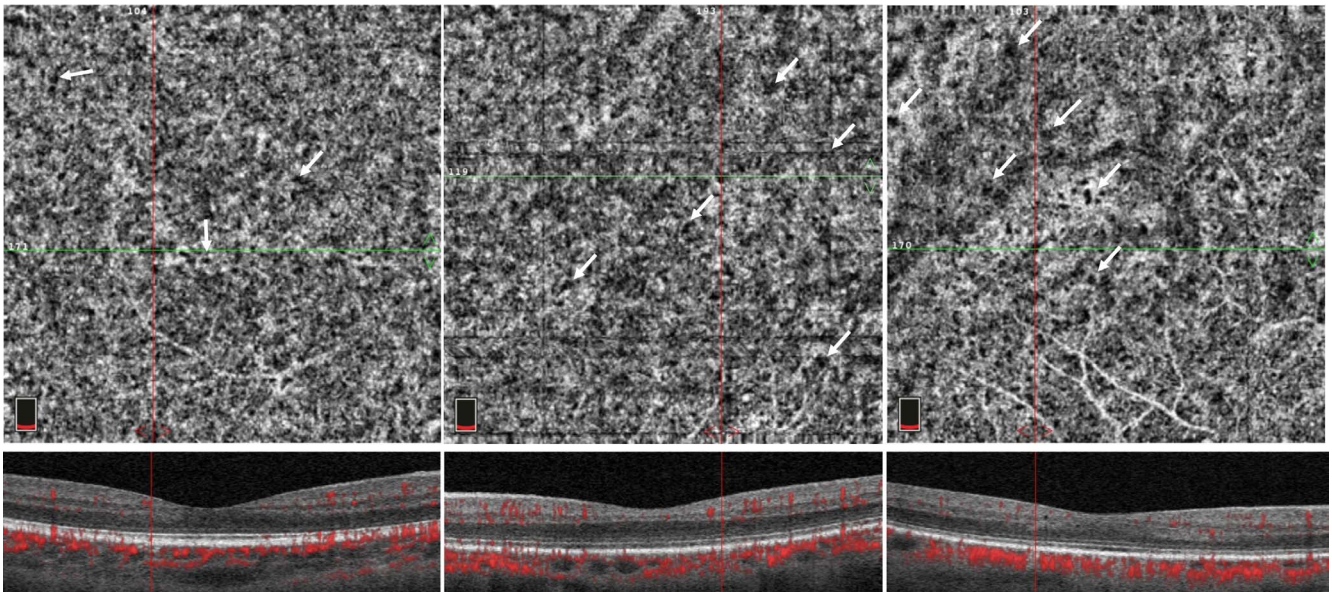

Figure 2. En face OCTA and corresponding OCT cross-sectional B-scan overlay illustrating larger CC flow void area in eyes with progressive myopia. *Left*, CC en face image of a 41-year-old male patient with high myopia. Refractive error was –6 D, total number of flow voids was 95, total area of flow void was 3.423 mm², and average area of flow void was 0.010 mm². *Middle*, CC en face image of a 55-year-old female patient with high myopia. Refractive error was –9 D, total number of flow voids was 77, total area of flow void was 3.529 mm², and average area of flow void was 0.020 mm². *Right*, CC en face image of a 61-year-old female patient with high myopia. The refractive error was –10.5 D, total number of flow voids was 67, total area of flow void was 3.525 mm², and average area of flow void was 0.025 mm². The illustrated *green* and *red lines* each intersect at an area of flow void. The corresponding B scan illustrates the absence of a corresponding flow overlay signal at the *vertical red line*. The *white arrows* represent additional areas of flow void. Note the increasing flow void area with increasing myopic refractive error.

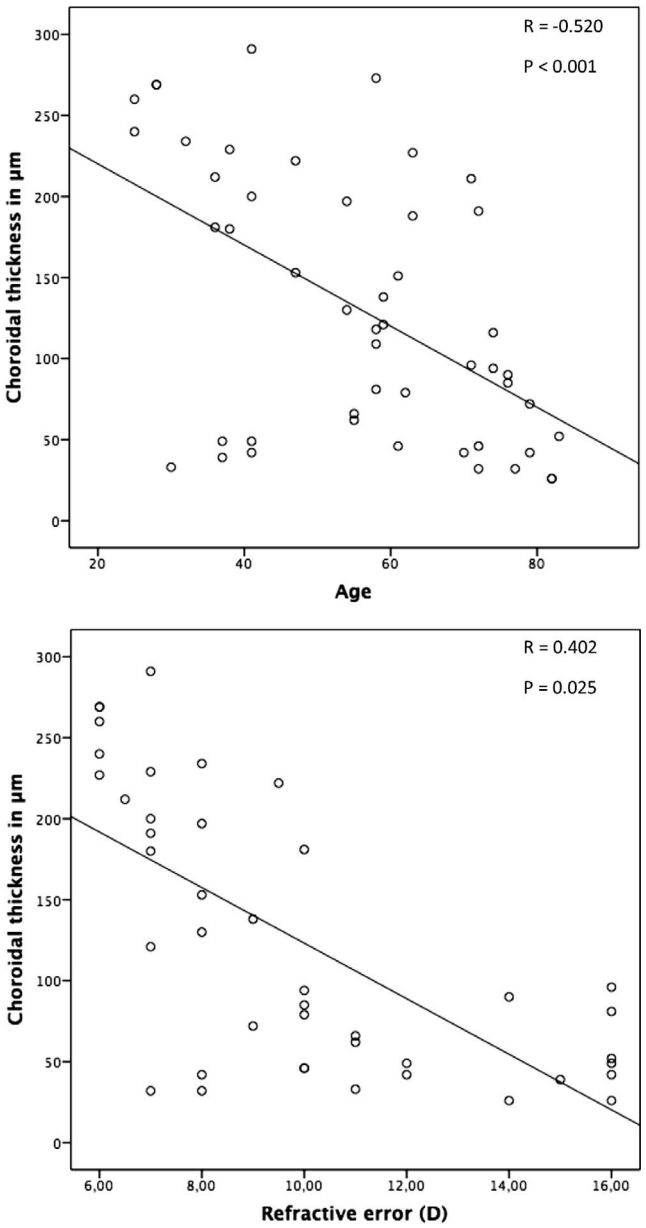

FIGURE 3. Correlation between choroidal thickness as the dependent variable versus age and refractive error. *Upper*, simple scatter plot of age (*x*-axis) versus choroidal thickness in micrometer (*y*-axis), $R = -0.520$, $P < 0.001$. *Lower*, simple scatter plot of refractive error in diopters (*x*-axis) versus choroidal thickness in micrometer (*y*-axis), $R = 0.402$, $P = 0.025$. Age and refractive error are negatively correlated with choroidal thickness.

findings with decreased retinal blood flow and vessel diameter in eyes with high myopia using laser Doppler velocimetry. In our study, we used FD as a measure of vessel complexity and branching, and both the SCP and DCP showed statistically significant lower complexity compared with the control group. It has been speculated that excessive axial elongation of the eyeball in highly myopic eyes can cause biomechanical stretching of the retina, choroid, and sclera.[32,33] This mechanical stretching may cause straightening and narrowing of the vessels and reduction of the associated branching in highly myopic eyes.

Our study identified measurable flow alteration in the CC associated with myopia. We found a decreased total number of flow voids, but an increase in the average and total flow void area versus the control group. These results confirmed previous work using histologic techniques. In an animal model, Hirata and Negi[34] reported a decreased density and capillary diameter in the CC of myopic eyes studied with scanning electron microscopy. They also reported an increase in the distance between adjacent intercapillary meshes of the CC. They attributed the decrease in CC density to capillary thinning observed with transmission electron microscopy. In another study, Shih et al.[18] demonstrated reduced choroidal blood flow in chicks with induced myopia due to visual deprivation. The authors attributed the reduced choroidal blood flow to the ocular enlargement of myopic eyes leading to choroidal stretching and thinning. The authors also noted that choroidal blood flow might be reduced as an adaptive response to myopia-induced thinning of the retina. The normal high flow is known to be essential to provide oxygen and nutrients to the outer retina; however, with myopia-induced retinal thinning, choroidal flow may be reduced to sustain the outer retina.[18,35] We cannot, however, exclude the possibility that the alterations in the area of the CC may be simply the result of expansion or stretching of the CC that would occur with increased axial enlargement and myopia as opposed to frank choroidal loss or atrophy.

In addition, in an in vivo study using color Doppler ultrasonography, another group illustrated a decrease in the choroidal blood flow in degenerative myopia and attributed this reduction to increased vascular resistance and narrowing in the posterior ciliary artery.[15] James et al.[36] reported that choroidal blood flow in myopic eyes was decreased as the axial length increased using ocular blood flow computerized tonometry. Recently, using OCTA, Spaide[10] identified a systematic reduction in CC flow characterized by increasing areas of flow void that correlated with age. In his cohort, the areas of flow void were reduced in number but increased in size according to age and hypertension, very similar to our findings that were correlated with myopia, and indicating that CC flow alteration may be a mechanism of aging.[10]

As with previous studies,[37–39] choroidal thickness in myopic eyes in our cohort was statistically significantly lower than in the control group, but we found no correlation between the choroidal thickness and the quantitative features of CC flow, such as total and average size of flow void area. However, the refractive error demonstrated a weak correlation with total and average flow void area in the CC. This finding might indicate that the choroidal thinning may be secondary to ocular elongation,[40] and the perfusion of the CC may be an independent factor.

In our cohort, six eyes with high myopia had LC, seven eyes were complicated by myopic CNV, and one eye showed CC atrophy. There was a significant correlation between total area of flow void in the CC and the presence of LC. Lacquer cracks are believed to be breaks in the RPE–Bruch's membrane complex caused by stretching of the eyeball and axial elongation. However, a previous study failed to demonstrate an association of LC with axial elongation.[41] The formation of LC was considered a risk factor for developing CNV and patchy chorioretinal atrophy, although the relationship between LCs and CNV development remains unclear.[42] Ohno-Matsui and Tokoro[43] reported the development of patchy chorioretinal atrophy adjacent to LC formation in eyes with longer axial length and described choroidal filling delay at the posterior pole, which appeared at the peripheral end of the LC due to mechanical stress from axial elongation. Our results showed an increased total area of flow void in myopic eyes, and a positive correlation with LC number may indicate that CC ischemia could be related to LC formation. The small number of cases with LC formation limits the power of this study to make

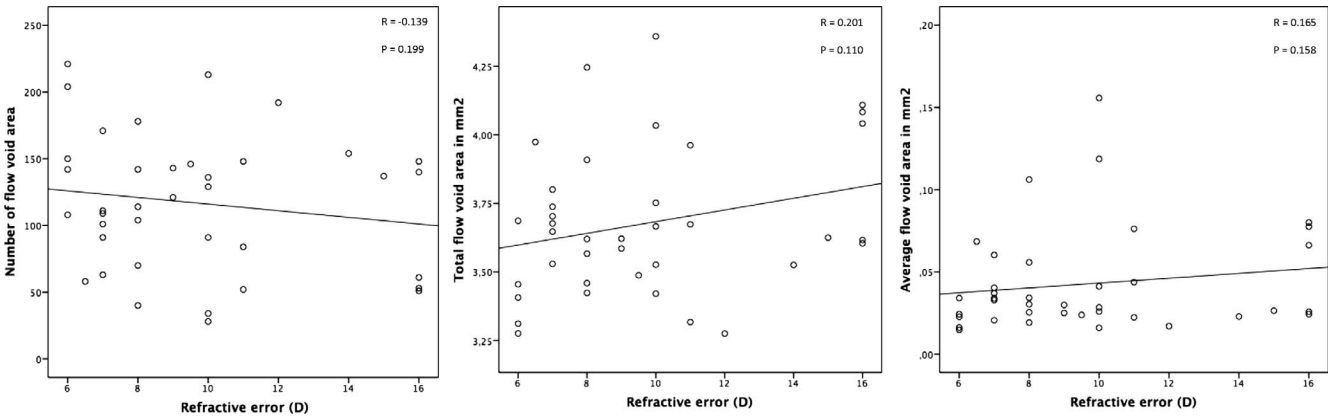

FIGURE 4. Correlation between refractive error as the dependent variable and quantitative parameters of the CC as independent variable. The refractive error in diopters is represented on the *x*-axis as a dependent variable in each graph. *Left*, simple scatter with the total number of flow voids (*y*-axis), $R = -0.139$, $P = 0.199$. *Middle*, simple scatter plot with total flow void area in mm^2 (*y*-axis), $R = 0.201$, $P = 0.110$. *Right*, simple scatter plot with the average flow void area in mm^2 (*y*-axis), $R = 0.165$, $P = 0.158$. Although the total number of flow voids is negatively correlated with refractive error, the total and average flow void areas are positively correlated.

definitive conclusions. Further studies are necessary to address these relationships.

Our study had a number of strengths and is one of the first investigations to describe the quantitative microvascular features of the retina and CC in progressively myopic eyes using OCTA. Further, this cross-sectional study included an age-matched control group. Moreover, flow characteristics of the CC measured by OCTA confirmed previous histopathologic techniques, which have not been previously demonstrated in vivo.

It also should be noted that the present study has limitations. First, the relatively small sample size of this study may limit our ability to make definitive conclusions correlating quantitative features of the CC versus the various pathologic changes in myopia. Second, we lacked axial length data to correlate with quantitative features of CC flow. In addition, the OCTA technique used in this study has limitations including motion and projection artifact and segmentation error. The use of a spectral-domain device can be associated with greater signal sensitivity roll-off that can affect the quantitative measurement of deeper tissues, such as the CC. Myopic eyes in our study did show a significantly lower signal strength score compared with the control group; however, the association between the signal strength and quantitative features of the CC was not statistically significant. Flow void areas in the CC may represent areas of no flow or areas of flow lower than the detectable threshold of the OCTA instrument, which could explain the high value for the area of flow void in our cohort. We attempted to reduce the impact of artifact on our quantitative analysis by using the method previously described by Spaide.[10] Specifically, we adjusted the segmentation level of the CC slab 34 μm below the RPE to minimize projection artifact, and we excluded cases with retinal or RPE pathology that could cause signal attenuation roll-off.[10] In addition, eyes with myopic CNV and atrophy of the RPE–Bruch's membrane complex or CC were excluded from the quantitative analysis to eliminate potential shadowing effects of CNV on the CC and to avoid the unmasking effect of CC loss that may cause greater visibility of the deeper choroidal vessels.

In conclusion, our study using OCTA demonstrated reduced VD in the retina of eyes with high myopia and an increase in the total and average area of flow voids in the CC. Whether the apparently reduced retinal and CC perfusion in eyes with high myopia is a cause or result of other associated pathologic abnormalities needs to be investigated in future studies. Optical coherence tomography angiography imaging of the microvasculature of the CC has the potential to become a simple, noninvasive, and practical technique for the informative evaluation and understanding of the underlying mechanisms of various pathologic changes related to myopia, such as LC, atrophy, and myopic CNV.

Acknowledgments

Supported by The Macula Foundation, Inc., New York, NY, USA.

Disclosure: **M. Al-Sheikh**, None; **N. Phasukkijwatana**, None; **R. Dolz-Marco**, Alcon (F), Allergan (F), Bayer (F), Heidelberg Engineering (F), Novartis (F), Thea (F); **M. Rahimi**, None; **N.A. Iafe**, None; **K.B. Freund**, Genentech (C), Optos (C), Optovue (C), Heidelberg Engineering (C), Bayer HealthCare (C); **S.R. Sadda**, Optos (C, F), Carl Zeiss Meditec (C, F), Allergan (C, F), Genentech (C, F), Thrombogenics (C), Novartis (C), Iconic (C); **D. Sarraf**, Novartis (C, S), Optovue (C, S), Bayer (C), Genentech (C, F), Optovue (C, F), Allergan (F), Heidelberg (F), Regeneron (F)

References

1. Nagiel A, Sadda SR, Sarraf D. A promising future for optical coherence tomography angiography. *JAMA Ophthalmol*. 2015;133:629–630.
2. Spaide RF, Klancnik JM Jr, Cooney MJ. Retinal vascular layers imaged by fluorescein angiography and optical coherence tomography angiography. *JAMA Ophthalmol*. 2015;133:45–50.
3. Jia Y, Tan O, Tokayer J, et al. Split-spectrum amplitude-decorrelation angiography with optical coherence tomography. *Opt Express*. 2012;20:4710–4725.
4. Al-Sheikh M, Akil H, Pfau M, Sadda SR. Swept-source oct angiography imaging of the foveal avascular zone and macular capillary network density in diabetic retinopathy. *Invest Ophthalmol Vis Sci*. 2016;57:3907–3913.
5. Iafe NA, Phasukkijwatana N, Chen X, Sarraf D. Retinal capillary density and foveal avascular zone area are age-dependent: quantitative analysis using optical coherence tomography angiography. *Invest Ophthalmol Vis Sci*. 2016; 57:5780–5787.
6. Klufas M, Phasukkijwatana N, Iafe N, et al. Optical coherence tomography angiography reveals choriocapillaris flow reduction in placoid chorioretinitis. *Ophthalmology Retina*. 2016; 1:77–91.

7. Kuehlewein L, Bansal M, Lenis TL, et al. Optical coherence tomography angiography of type 1 neovascularization in age-related macular degeneration. *Am J Ophthalmol*. 2015;160:739–748.e2.
8. Nemiroff J, Kuehlewein L, Rahimy E, et al. Assessing deep retinal capillary ischemia in paracentral acute middle maculopathy by optical coherence tomography angiography. *Am J Ophthalmol*. 2016;162:121–132.e1.
9. Phasukkijwatana N, Iafe N, Sarraf D. Optical coherence tomography angiography of a29 birdshot chorioretinopathy complicated by retinal neovascularization. *Retin Cases Brief Rep*. 2016;11(suppl 1):S68–S72.
10. Spaide RF. Choriocapillaris flow features follow a power law distribution: implications for characterization and mechanisms of disease progression. *Am J Ophthalmol*. 2016;170:58–67.
11. Zahid S, Dolz-Marco R, Freund KB, et al. Fractal dimensional analysis of optical coherence tomography angiography in eyes with diabetic retinopathy. *Invest Ophthalmol Vis Sci*. 2016;57:4940–4947.
12. Sperduto RD, Seigel D, Roberts J, Rowland M. Prevalence of myopia in the United States. *Arch Ophthalmol*. 1983;101:405–407.
13. Moriyama M, Ohno-Matsui K, Hayashi K, et al. Topographic analyses of shape of eyes with pathologic myopia by high-resolution three-dimensional magnetic resonance imaging. *Ophthalmology*. 2011;118:1626–1637.
14. Rahimy E, Beardsley RM, Gomez J, Hung C, Sarraf D. Grading of posterior staphyloma with spectral-domain optical coherence tomography and correlation with macular disease. *Can J Ophthalmol*. 2013;48:539–545.
15. Akyol N, Kukner AS, Ozdemir T, Esmerligil S. Choroidal and retinal blood flow changes in degenerative myopia. *Can J Ophthalmol*. 1996;31:113–119.
16. Benavente-Perez A, Hosking SL, Logan NS, Broadway DC. Ocular blood flow measurements in healthy human myopic eyes. *Graefes Arch Clin Exp Ophthalmol*. 2010;248:1587–1594.
17. Shimada N, Ohno-Matsui K, Harino S, et al. Reduction of retinal blood flow in high myopia. *Graefes Arch Clin Exp Ophthalmol*. 2004;242:284–288.
18. Shih YF, Fitzgerald ME, Norton TT, Gamlin PD, Hodos W, Reiner A. Reduction in choroidal blood flow occurs in chicks wearing goggles that induce eye growth toward myopia. *Curr Eye Res*. 1993;12:219–227.
19. La Spina C, Corvi F, Bandello F, Querques G. Static characteristics and dynamic functionality of retinal vessels in longer eyes with or without pathologic myopia. *Graefes Arch Clin Exp Ophthalmol*. 2016;254:827–834.
20. Alten F, Heiduschka P, Clemens CR, Eter N. Exploring choriocapillaris under reticular pseudodrusen using OCT-angiography. *Graefes Arch Clin Exp Ophthalmol*. 2016;254:2165–2173.
21. Nesper PL, Soetikno BT, Fawzi AA. Choriocapillaris non-perfusion is associated with poor visual acuity in eyes with reticular pseudodrusen. *Am J Ophthalmol*. 2017;174:42–55.
22. Ohno-Matsui K. What is the fundamental nature of pathologic myopia [published online ahead of print October 11, 2016]. *Retina*. doi:10.1097/IAE.0000000000001348.
23. Kraus MF, Liu JJ, Schottenhamml J, et al. Quantitative 3D-OCT motion correction with tilt and illumination correction, robust similarity measure and regularization. *Biomed Opt Express*. 2014;5:2591–2613.
24. Kraus MF, Potsaid B, Mayer MA, et al. Motion correction in optical coherence tomography volumes on a per a-scan basis using orthogonal scan patterns. *Biomed Opt Express*. 2012;3:1182–1199.
25. Spaide RF, Fujimoto JG, Waheed NK. Image artifacts in optical coherence tomography angiography. *Retina*. 2015;35:2163–2180.
26. Wang Q, Chan S, Yang JY, et al. Vascular density in retina and choriocapillaris as measured by optical coherence tomography angiography. *Am J Ophthalmol*. 2016;168:95–109.
27. Yang Y, Wang J, Jiang H, et al. Retinal microvasculature alteration in high myopia. *Invest Ophthalmol Vis Sci*. 2016;57:6020–6030.
28. Schneider CA, Rasband WS, Eliceiri KW. NIH Image to ImageJ: 25 years of image analysis. *Nat Methods*. 2012;9:671–675.
29. Masters BR. Fractal analysis of the vascular tree in the human retina. *Annu Rev Biomed Eng*. 2004;6:427–452.
30. Phansalkar N, More S, Sabale A, Joshi M. Adaptive local thresholding for detection of nuclei in diversely stained cytology images. *Proc International Conf Commun Signal Process*. 2011;154:218–220.
31. Tokoro T. On the definition of pathologic myopia in group studies. *Acta Ophthalmol Suppl*. 1988;185:107–108.
32. Lam DS, Leung KS, Mohamed S, et al. Regional variations in the relationship between macular thickness measurements and myopia. *Invest Ophthalmol Vis Sci*. 2007;48:376–382.
33. Wu PC, Chen YJ, Chen CH, et al. Assessment of macular retinal thickness and volume in normal eyes and highly myopic eyes with third-generation optical coherence tomography. *Eye (Lond)*. 2008;22:551–555.
34. Hirata A, Negi A. Morphological changes of choriocapillaris in experimentally induced chick myopia. *Graefes Arch Clin Exp Ophthalmol*. 1998;236:132–137.
35. Yancey CM, Linsenmeier RA. The electroretinogram and choroidal po2 in the cat during elevated intraocular pressure. *Invest Ophthalmol Vis Sci*. 1988;29:700–707.
36. James CB, Trew DR, Clark K, Smith SE. Factors influencing the ocular pulse–axial length. *Graefes Arch Clin Exp Ophthalmol*. 1991;229:341–344.
37. Flores-Moreno I, Lugo F, Duker JS, Ruiz-Moreno JM. The relationship between axial length and choroidal thickness in eyes with high myopia. *Am J Ophthalmol*. 2013;155:314–319.e1.
38. Gupta P, Saw SM, Cheung CY, et al. Choroidal thickness and high myopia: a case-control study of young chinese men in singapore. *Acta Ophthalmol*. 2015;93:e585–e592.
39. Ohsugi H, Ikuno Y, Oshima K, Tabuchi H. 3-d choroidal thickness maps from EDI-OCT in highly myopic eyes. *Optom Vis Sci*. 2013;90:599–606.
40. Wang S, Wang Y, Gao X, Qian N, Zhuo Y. Choroidal thickness and high myopia: a cross-sectional study and meta-analysis. *BMC Ophthalmol*. 2015;15:70.
41. Curtin BJ, Karlin DB. Axial length measurements and fundus changes of the myopic eye. *Am J Ophthalmol*. 1971;71:42–53.
42. Ikuno Y, Sayanagi K, Soga K, et al. Lacquer crack formation and choroidal neovascularization in pathologic myopia. *Retina*. 2008;28:1124–1131.
43. Ohno-Matsui K, Tokoro T. The progression of lacquer cracks in pathologic myopia. *Retina*. 1996;16:29–37.

Investigative Ophthalmology & Visual Science